Total lightning activity as an indicator of updraft characteristics

Wiebke Deierling[1] and Walter A. Petersen[2]

Received 13 November 2007; revised 14 April 2008; accepted 28 April 2008; published 28 August 2008.

[1] This study investigates the relationship of total lightning activity and updraft characteristics, such as updraft volume and maximum updraft speed, for a number of storms of different types occurring in the High Plains and in Northern Alabama. Ground-based Doppler and dual polarimetric radar observations were used to compute updraft characteristics. Also, ground-based total lightning data were available at both locations. Results show that time series of updraft volume in the charging zone (at temperatures colder than $-5°C$) with vertical velocities greater than either 5 or 10 m s^{-1} have clear relationships with total lightning activity ($r = 0.93$). Furthermore, these relationships between updraft volume and lightning activity for the storm types of the two climate regimes tend to converge when considering only the subfreezing layers of the clouds. Neither the maximum nor the mean updraft speed correlate as well with total lightning activity ($r = <0.8$) as updraft volume. Through expanded study designed to explore further regime variability (or lack thereof) of updraft volume-lightning flash rate relationships, better or refined parameterizations for the numerical forecasting of lightning and/or detection and prediction of storm intensity could be realized.

Citation: Deierling, W., and W. A. Petersen (2008), Total lightning activity as an indicator of updraft characteristics, *J. Geophys. Res.*, *113*, D16210, doi:10.1029/2007JD009598.

1. Introduction

[2] Lightning flashes occur as discrete entities that are relatively easy to detect and count with high temporal and spatial resolution over large ranges and regions of limited weather data availability (e.g., over complex terrain, oceans etc.). In recent years, the development and deployment of several lightning detection systems such as the space-borne Tropical Rainfall Measurement Mission (TRMM) Lightning Imaging Sensor (LIS) [*Christian et al.*, 1999], and modern ground-based VHF Lightning Mapping Arrays (LMA) [*Thomas et al.*, 2004] have increased the availability of total lightning measurements significantly. The availability and coverage of these data may increase even more dramatically with the deployment of the Geostationary Lightning Mapper (GLM), currently scheduled to fly on the next generation of Geostationary Operational Environmental Satellites (GOES-R) [*Christian*, 2008]. The ability of future instruments such as the GLM to provide continuous temporal and broad spatial (hemispheric) sampling of total lightning and attendant hazardous weather conditions (i.e., thunderstorms) provides strong motivation for quantitatively defining useful physical relationships between lightning characteristics and microphysical and dynamical storm parameters.

[3] As relationships between lightning flash characteristics and thunderstorm kinematic and microphysical parameters become better defined, lightning information can be better incorporated into mainstream meteorological applications including warning decision support [e.g., *Goodman et al.*, 2005] and improved numerical weather prediction [*McCaul et al.*, 2006; *Mansell et al.*, 2007]. To this end, the objective of this paper is to investigate storm scale relationships between total lightning flash rate and thunderstorm kinematic characteristics such as updraft volume and maximum updraft speed. These relationships are summarized for a collection of thunderstorms observed in the distinctly different climates of the Colorado/Kansas High Plains and subtropical northern Alabama using ground-based dual-Doppler and dual-polarimetric radar together with VHF total lightning data.

[4] Many field observations [*Workman and Reynolds*, 1949; *Williams and Lhermitte*, 1983; *Dye et al.*, 1989; *Rutledge et al.*, 1992; *Carey and Rutledge*, 1996; *Petersen et al.*, 1996, 1999] suggest that in-cloud mixed phase microphysics ($0°C$ to $-40°C$) driven by the presence of a strong low to midlevel updraft [e.g., >6 m s^{-1} in the mean; *Zipser and Lutz*, 1994] are necessary to facilitate significant cloud electrification and the strong electric fields required to initiate lightning. This juxtaposition of updraft and mixed phase microphysics provides a region where noninductive charging can efficiently occur via rebounding collisions between graupel/hail and ice crystals in the presence of supercooled liquid water [*Reynolds et al.*, 1957; *Takahashi*, 1978; *Jayaratne et al.*, 1983; *Saunders et al.*, 1991; *Saunders and Peck*, 1998; *Takahashi and Miyawaki*, 2002; *Mansell et al.*, 2005].

[5] More specifically, the updraft is a key component of the electrical generator because it drives the development of graupel and ice crystals, enhances particle collision frequen-

[1]National Center for Atmospheric Research, Boulder, Colorado, USA.
[2]ESSC/NSSTC University of Alabama in Huntsville, Huntsville, Alabama, USA.

0148-0227/08/2007JD009598

cies at updraft boundaries, and, in cooperation with gravitational forces, provides a means to separate charge on the cloud scale enabling, for example, the formation of gravitationally driven precipitation currents. Thus one expects a correlation to exist between total lightning activity and updraft characteristics. Indeed, theory-based arguments advanced by *Boccippio* [2002] suggest that thunderstorm generator power is linearly related to lightning activity (current) and also to the product of generator current density and thunderstorm size. Since generator current density ($C\ s^{-1}\ m^{-2}$) is the product of charge density (Cm^{-3}) and charge transport velocity ($m\ s^{-1}$), both updraft area and magnitude are directly related to the total generator electrical power.

[6] Indeed, updraft–total lightning relationships of individual thunderstorms have been explored in several previous publications [e.g. *Lang and Rutledge*, 2002; *Tessendorf et al.*, 2005; *Wiens et al.*, 2005]. *Tessendorf et al.* [2005] and *Wiens et al.* [2005] generally found good correlations between the volume of updraft exceeding 10 $m\ s^{-1}$ and total lightning activity. *Lang and Rutledge* [2002] investigated the kinematic characteristics of thunderstorms accompanied by a low percentage of cloud-to-ground flashes and thunderstorms that predominantly produced positive cloud-to-ground (PPCG) flashes. Their work suggests that PPCG storms are accompanied by a larger area of stronger updrafts ($w > 20$ m/s), yielding more condensate, more charge-separating collisions between ice hydrometeors, and subsequently a greater reservoir of charge (e.g. greater reservoir of lower positive charge in terms of the PPCG storms). More recent modeling studies also suggest a good correlation between updraft volume and total lightning for at least one severe thunderstorm case simulated [*Kuhlman et al.*, 2006].

[7] In this study we extend previous observational and modeling results via the examination of updraft and lightning characteristics for a broader set of thunderstorm cases observed in both midlatitude and subtropical environments. The following sections describe the data used (section 2), methodologies used to retrieve three dimensional wind fields, updraft characteristics, and total lightning (section 3), and finally the results relating updraft characteristics such as volume and magnitude to total lightning activity (section 4). We conclude the study with a brief summary (section 5).

2. Data

[8] To investigate the relationship between total lightning and thunderstorm kinematic characteristics such as updraft volume and maximum updraft speed, data collected for different types of thunderstorms (single cell, multicell and supercell) in Northern Alabama during 2005 were used as well as data from two field projects that took place in the High Plains of Colorado/Kansas – one is the Stratospheric–Tropospheric Experiment: Radiation, Aerosols and Ozone (STERAO-A) [*Dye et al.*, 2000], the other one the Severe Thunderstorm Electrification and Precipitation Study (STEPS) [*Lang et al.*, 2004]. A list of thunderstorms that have been investigated in this study, including a short description of the storms, storm duration, number of radar volumes that were used in this study etc., is given in Table 1. Note that not all storms could be observed throughout their entire lifetime, since some storms moved in or out of the observational domain.

[9] During STERAO-A radar data was collected from the Colorado State University–Chicago-Illinois State Water Survey (CSU-CHILL) National Radar Facility's S-band radar [*Brunkow et al.*, 2000]. For STERAO-A no other ground-based radar data were available for dual-Doppler analysis, hence the three-dimensional wind field was estimated using a four-dimensional variational approach described below. During STERAO-A, total lightning data was collected from the Office Nationale d'Etudes et de Recherches Aerospatiales (ONERA) three-dimensional lightning VHF-interferometer system [*Laroche et al.*, 1994; *Defer et al.*, 2001].

[10] During STEPS dual-Doppler polarimetric radar data were collected by the CSU-CHILL and the National Center for Atmospheric Research (NCAR) S-band dual polarimetric (S-Pol) radar [*Keeler et al.*, 2000]. These two research radars together with the Goodland, Kansas National Weather Service (NWS) Weather Surveillance Radar-1988 Doppler (WSR-88D) radar formed a triangle with approximately 60 km baselines and performed synchronized volume scans allowing retrieval of the three-dimensional wind fields via dual or triple Doppler wind analyses. Total lightning activity in the STEPS domain was observed using the deployable LMA of the New Mexico Institute of Mining and Technology (NMIMT) [*Thomas et al.*, 2004].

[11] In northern Alabama dual-Doppler radar data were collected using the University of Alabama Huntsville/National Space Science and Technology Center (UAH/NSSTC) dual polarimetric C-band Doppler radar, ARMOR [Advanced Radar for Meteorological and Operational Research; *Petersen et al.*, 2005] and the nearby Hytop National Weather Service WSR-88D radar (68 km baseline). Because C-band radars such as ARMOR suffer from significant attenuation in heavy rain or large hail events, radar reflectivity and differential reflectivity measured by ARMOR were corrected for attenuation and differential attenuation using locally modified software originally developed for/used by the Bureau of Meteorology Research Centre (BMRC) C-pol radar, and based on techniques described in *Bringi et al.* [2001]. The total lightning data were collected using the North Alabama LMA, which is permanently installed in the Huntsville, AL area [*Goodman et al.*, 2005].

3. Methodology

[12] Both in-cloud (IC) and cloud-to-ground (CG) flashes consist of various components which emit electromagnetic radiation in a broad band. Some of these flash components such as recoil streamers, negative stepped leaders or dart leaders and sometimes return strokes emit strongly in the VHF frequency domain [e.g., *Defer et al.*, 2001]. Both, the ONERA lightning mapper as well as the LMA detect impulsive VHF sources emitted from these components of lightning flashes. In order to determine a flash rate, measured VHF sources have to be grouped into flashes by applying spatial and temporal constraints. Herein, total flash rate from the ONERA lightning mapper was determined by *Defer et al.* [2001] using two techniques, the so called XYZ

Table 1. List of Thunderstorms That Have Been Investigated in This Study

Date	Location	Storm Type	Short Description	Number of Radar Volumes	Start and End Time of Radar Volumes in (h/min) UTC	Number of Tilts in the Radar Volumes and Their Average Duration	Lightning Detection System, Radars	Method to Retrieve Vertical Velocity
5 July 2000	STEPS	Supercell thunderstorm [*Lang et al.*, 2004; *MacGorman et al.*, 2005]	Supercell Storm had a funnel cloud, hail reports of 2.5 and 4.3 cm hail from SPC and 33 m/s gusts [*Lang et al.*, 2004]	27	22:39–01:22 (6 July 2000)	CHILL: sector scans with 21–24 tilts, 3.5 min SPOL: sector scans with 17–22 tilts, 3.5 min; KGLD: 14 tilts, 4.5 min	LMA, CSU-CHILL radar, SPOL-radar, Goodland WSR-88D	Dual-dopper retrieval (downward integration)
5 July 2000	STEPS	Supercell thunderstorm [*Lang et al.*, 2004; *MacGorman et al.*, 2005]	Supercell thunderstorm	22	22:52–00:56 (6 July 2000)	CHILL: sector scans with 21–24 tilts, 3.5 min SPOL: sector scans with 17–22 tilts, 3.5 min KGLD: 14 tilts, 4.5 min	LMA, CSU-CHILL radar, SPOL-radar, Goodland WSR-88D	Dual-dopper retrieval (downward integration)
10 July 1996	STERAO-A	One multicell storm evolving to a supercell storm [*Dye et al.*, 2000]	No large hail or strong winds reported	18	22:47–02:30 (11 July 1996)	CHILL: sector scans with around 18–23 tilts, 4–6 min	Onera interferometric lightning mapper, CSU-CHILL radar	VDRAS
6 June 2000	STEPS	Moderate intensity thunderstorm	No hail, wind or tornado reports	30	21:52–01:05 (7 June 2000)	CHILL: sector scans with 13–21 tilts, 3.5 min SPOL: sector scans with 15–21 tilts, 3.5 min KGLD: 14 tilts, 4.5 min	LMA, CSU-CHILL radar, SPOL-radar Goodland WSR-88D (KGLD)	Dual-dopper retrieval, variational scheme
6 June 2000	STEPS	Moderate intensity thunderstorm	No hail, wind or tornado reports	16	23:17–01:05 (7 June 2000)	CHILL: sector scans with 13–21 tilts, 3.5 min SPOL: sector scans with 15–21 tilts, 3.5 min KGLD: 14 tilts, 4.5 min	LMA, CSU-CHILL radar, SPOL-radar, Goodland WSR-88D	Dual-dopper retrieval, variational scheme
6 June 2000	STEPS	Weakly electrified single cell thunderstorm	No hail, wind or tornado reports	4	22:41–23:04	CHILL: sector scans with 13–21 tilts, 3.5 min SPOL: sector scans with 15–21 tilts, 3.5 min KGLD: 14 tilts, 4.5 min	LMA, CSU-CHILL radar, SPOL-radar, Goodland WSR-88D	Dual-dopper retrieval, variational scheme
21 February 2005	Northern Alabama	Severe storm, multicellular character	Several hail reports of 1.8 to 2.3 cm hail from SPC[a]	6	21:14–22:13	ARMOR: sector scan with 19 tilts, 8 min; KHTX: 14 tilts, 5 min	LMA, ARMOR and Hytop WSR-88D (KHTX)	Dual-dopper retrieval, variational scheme
7 April 2005	Northern Alabama	Moderate intensity ordinary thunderstorm, approaching severe	Hail report of 1.8 cm hail from SPC	9	19:18–20:17	ARMOR: sector scan with 18 tilts, 5.5 min KHTX: 14 tilts, 5 min	LMA, ARMOR and Hytop WSR-88D (KHTX)	Dual-dopper retrieval, variational scheme
13 July 2005	Northern Alabama	Single cell thunderstorm	No hail, wind or tornado reports	6	19:11–19:40	ARMOR: sector scan with 18 tilts, 3 min KHTX: 9 tilts, 5 min	LMA, ARMOR and Hytop WSR-88D (KHTX)	Dual-dopper retrieval, variational scheme
13 July 2005	Northern Alabama	Single cell thunderstorm	No hail, wind or tornado reports	8	20:30–21:15	ARMOR: sector scan with 18 tilts, 3.5 min KHTX: 9 tilts, 5 min	LMA, ARMOR and Hytop WSR-88D (KHTX)	Dual-dopper retrieval, variational scheme
13 July 2005	Northern Alabama	Single cell thunderstorm	No hail, wind or tornado reports	10	21:15–22:00	ARMOR: sector scan with 18 tilts, 3 min KHTX: 14 tilts, 5 min	LMA, ARMOR and Hytop WSR-88D (KHTX)	Dual-dopper retrieval, variational scheme

[a]SPC = Storm Prediction Center Reports from the National Oceanic and Atmospheric Administration (NOAA) and the National Weather Service (NWS).

analysis and additionally the angular analysis. In the XYZ analysis, VHF sources were assigned to flash components if their time difference was less than 200 μs and the velocity between the sources was lower than 10^8 m s^{-1}. The components were then assigned to a flash if the components last and first VHF sources were less than 250 ms and not more than 25 km apart. Additionally the whole flash duration could not exceed one second. For the angular analysis, flashes were determined manually by *Defer et al.* [2001] according to the azimuth, elevation and magnitude information of measured VHF sources from individual ONERA lightning mapper stations. The only criterion applied was that a VHF source is not allowed to belong to the same flash if it was recorded more than 0.5 s after the occurrence of the previous source. Note, that single sources with the time duration of 23 μs (which is the time resolution of the system) were allowed to count as one flash if they did not appear to be linked to another source. Total flash rate from the LMA was determined manually using visualization software from NMIMT [similar to *Defer et al.*, 2001] as well as with the inbuilt flash algorithm by NMIMT [*Thomas et al.*, 2003]. The algorithm applies the following constraints: VHF sources that were separated by not more than 150 ms in time, 3 km in horizontal distance and 5 km in the vertical were associated with the same flash [see *Thomas et al.*, 2003 or *Wiens et al.*, 2005].

[13] In order to retrieve updraft characteristics such as maximum updraft speed and updraft storm volumes dual Doppler syntheses were performed to compute three-dimensional wind fields of the investigated thunderstorms with the exception of the STERAO-A case. For this case (10 July 1996 storm) only single Doppler radar data from the CSU-CHILL radar were available. Here NCAR's Variational Doppler Radar Assimilation System (VDRAS) was used to calculate the three-dimensional wind fields [*Sun and Crook*, 1997, 2001; *Crook and Sun*, 2004]. First we will describe the dual-Doppler radar synthesis process, and then we will provide a short description of the VDRAS wind retrieval.

[14] Prior to synthesizing dual-Doppler winds, the radial velocity data from all radars involved in the analysis were thresholded by the minimum detectable power of the radars and de-aliased. For this task we used the NCAR SOLOII software. Noticeable contamination from sidelobes was removed manually with the SOLOII software. Ground clutter and second trip echoes were also removed with the help of the NCAR hydrometeor identification algorithm [*Vivekanandan et al.*, 1999] making use of polarimetric radar information (e.g. variances of differential reflectivity and phase measured by the CHILL, SPOL and ARMOR radars). In the next step, radar volumes collected at approximately the same time (at most two minutes apart from each other) from at least two radars were interpolated from radar space (spherical coordinate system) to a Cartesian grid using the NCAR REORDER software package. A Cressman filter weighting function was used for the conversion, employing a grid spacing in the x, y, z directions of 1 km with a radius of influence in accordance with the mean 'width' of the radar gates over the lifetime of the storms and the radar scanning strategy (usually around 1.2 km).

[15] In a third step, the combined gridded radar volumes were input into NCAR's Custom Editing and Display of Reduced Information in Cartesian Space (CEDRIC) [*Mohr et al.*, 1986] software package to perform the dual-Doppler wind synthesis and vertical velocity retrieval. Speed and direction of storm movement were accounted for in the synthesis. With two radars, the horizontal wind components, u and v (storm relative and non storm relative), can be determined directly. Vertical wind velocities are then calculated by employing a hydrometeor fallspeed relationship based on reflectivity and subsequently integrating the mass continuity equation. The mass continuity equation was integrated using three separate methods: integrating upward with a surface boundary condition, downward with a storm-top boundary condition, and variationally using both boundary conditions [*O'Brien*, 1970]. The calculations computed hydrometeor terminal fall speeds following *Marks and Houze* [1987], where the terminal fall speed (v_t) below the melting level is estimated as $v_t = 2.6 \cdot Z_h^{0.107}$ and above the melting level is estimated as $v_t = 0.817 \cdot Z_h^{0.063}$. Vertical velocities ($w$) were determined as the difference between the measured vertical velocities (W) from the solution of the mass continuity equation and a bulk estimate of the fall speed of precipitation particles (v_t) following $w = W - v_t$.

[16] Errors in the retrieval of vertical velocity can occur due to incorrect storm advection assumptions, boundary conditions (it is assumed that vertical velocities are zero at the upper and/or lower boundary), incomplete sampling of low-level divergence, and time differences between individual radar scans of two radars when sampling a storm. Time differences between PPI scans for the STEPS project were coordinated and usually within a few tenths of a minute. Time differences for the Northern Alabama cases were in a few cases as high as two minutes. Thus given an error of 1–2 m s^{-1} in estimates of the storm motion speed the total error in position is between 120 to 240 m. This error is below the resolution of the synthesis grid spacing of 1 km. Of course this does not address errors associated with temporal evolution of the storms during the periods of volume mismatch. Errors in boundary conditions (assuming $w = 0$ at the top of the storm and/or at the surface) and low-level divergence have different effects on the different integration schemes used to determine w [see *Matejka and Bartels*, 1998 for a review]. The upward integration scheme can be very unstable with respect to errors in low-level horizontal divergence and surface boundary conditions (the lowest sampled grid in the data may not fully reach the ground and $w = 0$ may not be representative). Errors in w grow with height when integrating from high densities to low densities and thus this method is most suitable for retrievals of w in the first few kilometers above the ground. The downward integration scheme is superior to the upward as the integration from lower to higher densities dampens errors in w that may be caused by errors in horizontal divergence. The variational integration scheme redistributes errors from both boundary conditions and can eliminate the errors caused by divergence incorrectly estimated or measured. Herein we use results from the variational integration scheme unless the lowest elevation scans from the radar were suspect. This situation occurred only once for the 5 July STEPS storms, and in that instance the downward integration yielded the most reasonable results (determined subjectively). Herein we also use horizontal divergence calculated from the two horizontal wind components.

Table 2. Linear Correlation Coefficients Between the Time Series of Mean Total Lightning Per Minute and Updraft Volumes[a]

	w_0	w_5	w_{10}	w_{20}	w_{max}	W_{mean}
Total Lightning	0.62 (0.1)	0.93 (0.87)	0.92 (0.85)	0.89 (0.8)	0.82 (0.68)	0.65 (0.69)

[a]With vertical velocities >0, 5, 10 and 20 m s^{-1} (w_0, w_5, w_{10}, and w_{20}) as well as maximum and mean updraft speeds (w_{max} and w_{mean}, respectively) above the −5°C level. The correlation coefficients of their total storm volume detrended counterparts are in brackets.

[17] The NCAR VDRAS system retrieves three-dimensional wind, temperature, pressure and microphysics fields from single or multi-Doppler radar observations. Here a time-dependent cloud scale model was fit to the time series of radar measurements (radial velocity and reflectivity) using a four dimensional variational (4DVAR) data assimilation technique [*Sun and Crook*, 1997]. *Sun and Crook* [1997] found that the VDRAS retrieval of a three-dimensional wind field with only single radar may lead to a noticeable increase in root mean square errors of the retrieved wind fields although their structures remained intact. For the STERAO-A case, VDRAS results (three-dimensional wind field structures) were inspected in detail and the trend of retrieved velocities considered correct [personal communications, A. Crook, 2005].

[18] Various measures of the updraft strength above the melting level where thunderstorm electrification takes place (e.g. above the −5°C level or limited only to the charging zone) were compared to total lightning activity. Herein the charging zone was roughly taken to be between −5°C to −40°C. Various measures of updraft strength include the mean updraft strength of all grid points with vertical velocities greater than 0 m s^{-1}, maximum updraft strength, and total updraft volumes with vertical velocities greater than 0, 5, 10 and 20 m s^{-1} (w_0, w_5, w_{10} and w_{20} in Table 2).

[19] Note, that radar measurements have a lower spatial (a few hundred meters to kilometers) and temporal resolution (order of several minutes) than lightning measurements (spatial resolution of tens to hundreds of meters and typical temporal resolution of on the order of 20–100 μs). Lightning also is a countable quantity whereas radar volume scans represent a sequence of time-integrated spatial "snapshots" from parts of thunderstorms. They give a measure of the "mean" updraft state over a radar volume time (duration of four to seven minutes). Thus when radar derived updraft characteristics were compared to total lightning measurements, the latter were combined using the mean amount of total lightning per minute over individual radar volume times in order to match the timescale of the radar measurements. Additionally, trends in the updraft characteristics and mean total lightning were removed from the total storm volume trend following *Wiens et al.* [2005] in order to take its influence out of the correlation.

4. Updraft Characteristics and Total Lightning

[20] In order to investigate the relationship between updraft characteristics for all eleven thunderstorms from the High Plains and Northern Alabama listed in Table 1, first measures for the updraft strength at altitudes above the −5°C level was compared to total lightning activity. The highest correlations were obtained using linear fits as compared to exponential, power law or logarithmic fits. Linear correlation coefficients between retrieved vertical velocity characteristics and mean total lightning activity as well as their by the storm volume detrended counterparts are presented in Table 2. These results generally suggest that updraft volumes with vertical velocities exceeding 0, 5, 10 and 20 m s^{-1} all correlate reasonably well with total lightning activity (linear correlation coefficients (r) ranging from 0.62 to 0.93). This is in agreement with *Lang and Rutledge* [2002] and *Wiens et al.* [2005].

[21] It is also interesting to note in Table 2 that the highest correlations were found between volumes of vertical velocity exceeding 5 m s^{-1} and 10 m s^{-1} in the "cold regions" of the storms *above the* −5°C *level* (w_5 and w_{10} respectively) and mean total lightning. *Zipser and Lutz* [1994] and *Petersen et al.* [1996, 1999] suggested that mean vertical velocities around 6–7 m s^{-1} in the layer from 0 to −20°C are needed to generate microphysical conditions conducive to lightning production in tropical thunderstorms. In this regard, the smaller regions of much higher updraft speed (e.g., w > 20 m s^{-1}) may not encompass the total updraft volume responsible for the most significant charge separation. Similarly the correlation between total lightning and maximum or mean updraft velocities appears weaker because they do not necessarily represent the volume of updraft velocities involved in both microscale and macroscale charge separation (see below). This may also be true for the updraft volumes with w > 0 m s^{-1}, which may include regions of updraft that may not contribute significantly to graupel growth and separation of charge.

[22] Scaling arguments summarized by *Boccippio* [2002] suggested that the updraft area should be related to the generator current density which in turn is linked to the electric activity of the storm. Following this train of thought, a reasonable explanation for the high correlation between updraft volume and lightning flash rate presented in Table 2 is that larger updraft volumes provide a larger source of condensate, thereby promoting the growth of larger precipitation particles such as graupel and hail, and also enabling the development of large cloud ice concentrations; i.e., provide the ingredients for a larger number of collisions and charge transfer between rimed graupel pellets and ice crystals. Consistent with this explanation, and to first order, updraft volume with w > 5 m s^{-1} and w > 10 m s^{-1} above the −5°C level should be well correlated with precipitation ice mass, independent of the two climate regime types. As an example, Figure 1 shows the updraft volume with w > 5 m s^{-1} and precipitation ice mass above the −5°C level (r = 0.91) on a logarithmic scale. The precipitation ice mass was computed using polarimetric radar data and appropriate reflectivity mass relationships as described in detail in *Deierling et al.* [2008]. Though the ice mass results were reported in separate studies [cf., *Deierling et al.*, 2008; *Latham et al.*, 2007], it is important to note that consistent with *Petersen et al.* [2005] a strong correlation was found to exist between precipitation ice mass and mean total lightning activity,

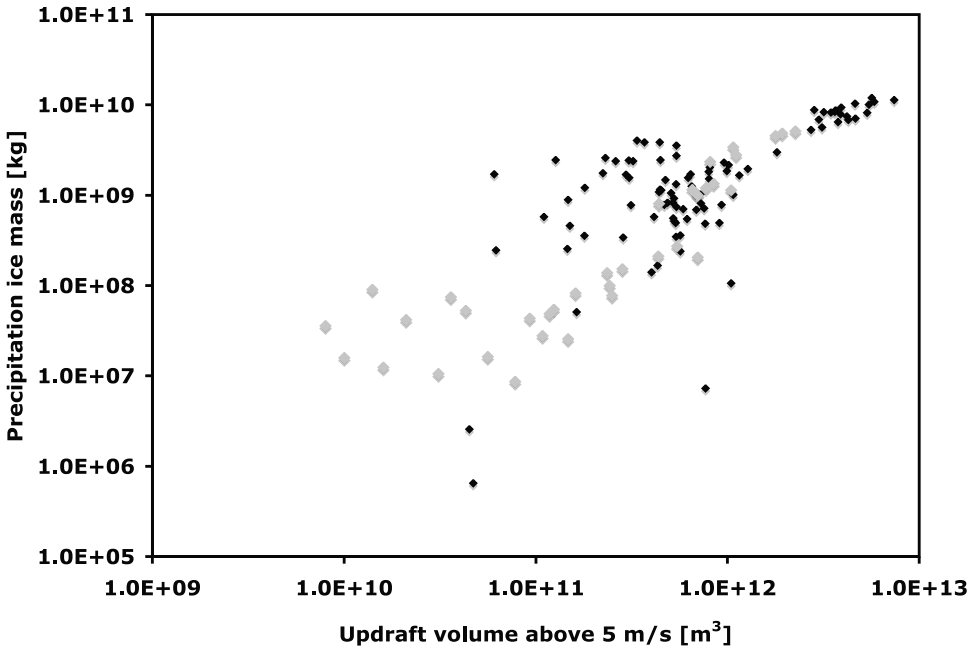

Figure 1. Updraft volume (m^3) above the −5°C level with velocities greater than 5 m s^{-1} versus precipitation ice mass (kg) for individual radar volumes of all eleven thunderstorms. The black dots mark data from the Colorado/Kansas High Plains, whereas the gray dots mark data from Northern Alabama.

where a linear fit represents best their relationship with a correlation coefficient of 0.94.

[23] To further elucidate trends between updraft volume and lightning (and by proxy, ice mass) discussed above and presented in Table 2, Figure 2 shows a scatter plot of w_5 versus mean total lightning activity. A linear least squares fit best represents the relationship between these two variables (r = 0.93). The linear fits and correlation coefficients for

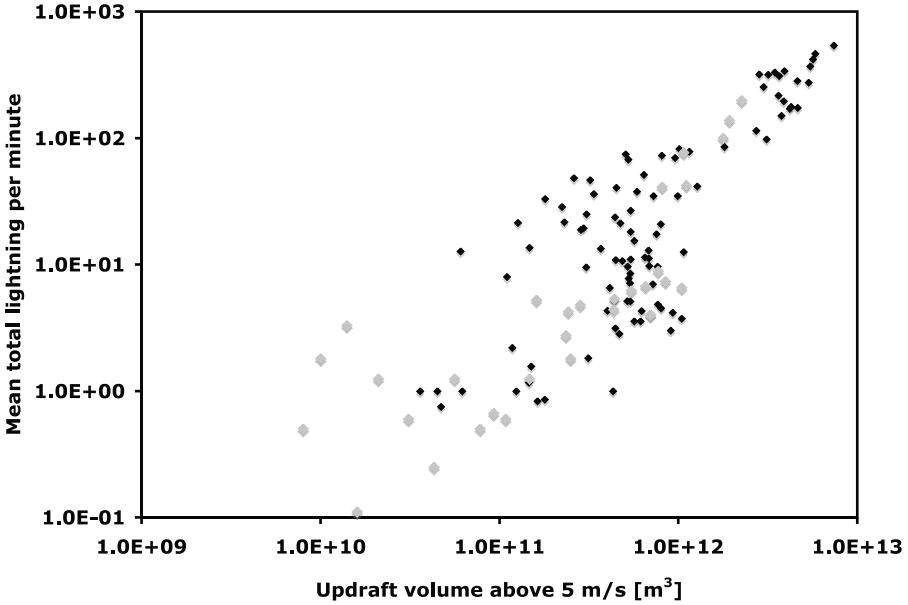

Figure 2. Updraft volume (m^3) above the −5°C level with velocities greater than 5 m s^{-1} versus mean total lightning per minute averaged over the radar volume time for individual radar volumes of all 11 thunderstorms. The black dots mark data from the Colorado/Kansas High Plains, whereas the gray dots mark data from Northern Alabama.

Table 3. Linear Fit of Mean Total Lightning Per Minute Averaged Over the Radar Volume Time Versus Updraft Volume (m^3) Above the −5°C Level With Velocities >5 m s^{-1}

	All Data Points	Data Points From Northern Alabama	Data Points From the Colorado/Kansas High Plains
Linear function	$f = 6.75 \times 10^{-11}\, w_5 - 13.9$	$f = 6.74 \times 10^{-11}\, w_5 - 14.3$	$f = 6.76 \times 10^{-11}\, w_5 - 13.7$
Correlation (r)	0.93	0.88	0.93

each of the High Plains and Alabama regions and also for the combined data set (all data points, regardless of region) are presented in Table 3. We see that both the linear fits and the correlations are all similar. Also, regardless of climate regime, higher flash rates are accompanied by a much lower scatter in updraft volume (Figure 2) indicating that the relationship between the two variables is more robust for storms associated with a larger volume of strong updraft.

[24] Because the updraft supplies condensate for ice processes (e.g., Figure 1) and the associated precipitation-based charging processes it is reasonable to suppose that the relationship between updraft magnitude and/or volume and lightning may vary as a function of the vertical structure of the updraft (i.e., as a function of the temperature layer where the updraft magnitude and volume are maximized). For example, robust mixed-phase ice processes, collision-based charging, and the concurrent ability to separate large masses of dissimilar sized electrically charged ice particles produced by these processes appear to be critical components in the electrification of thunderstorms. To meet these requirements it has been hypothesized that both the updraft size and strength must be sufficient in the right region of the cloud [e.g., *Zipser and Lutz*, 1994; *Petersen et al.*, 1996, 1999]. Hence establishment of a relationship between updraft magnitude/volume and lightning should consider the vertical draft structure as a function of temperature. To this end we expand on the results presented in Tables 2 and 3 and Figure 2 by examining the relationship between w_5 and total lightning activity in 10°C temperature (T) bands beginning at +10°C and extending above the melting level.

[25] As an illustration, we first consider the functional dependence between w_5 and lightning as a function of T, for T levels +10°C < T < 0°C and −20°C < T < −30°C respectively as a function of regime type (Figures 3a and 3b). In contrast to the regime similarity illustrated in Figure 2, results for the +10°C to 0°C layer (Figure 3a) suggest that for a given lightning amount corresponding updraft volumes tend to be *larger* for storms occurring in the subtropical Alabama region relative to that of the High Plains. Interestingly, if w_5 and lightning flash rates are subsequently compared for the subfreezing temperature layers of the active noninductive charging zone (e.g. Figure 3b), the relationship between w_5 and lightning flash rate becomes more similar between the regime types. That is, given that sufficient w_5 exists above the −10°C level, there appears to be less distinction in the electrical behavior between the two regimes – at least in terms of total lightning flash rate.

[26] The regime difference in behavior reflected in the warm cloud layer w_5 vs. lightning may simply reflect the impact of a more humid background and deeper warm-cloud layer combined with previously observed different updraft core properties in the southeast relative to the typical High Plains environment (i.e., cloud width and turbulent structure [*Musil and Smith*, 1989]). For example the combined impacts of enhanced water loading and entrainment in the warm cloud layer of southeastern storms may present a relative impediment to the production of lightning in *individual* southeastern U.S. thunderstorms; that is, a larger warm-cloud layer w_5 is required to supply the needed condensate (which may otherwise be depleted in warm-rain processes) for ice production and electrification. Conversely,

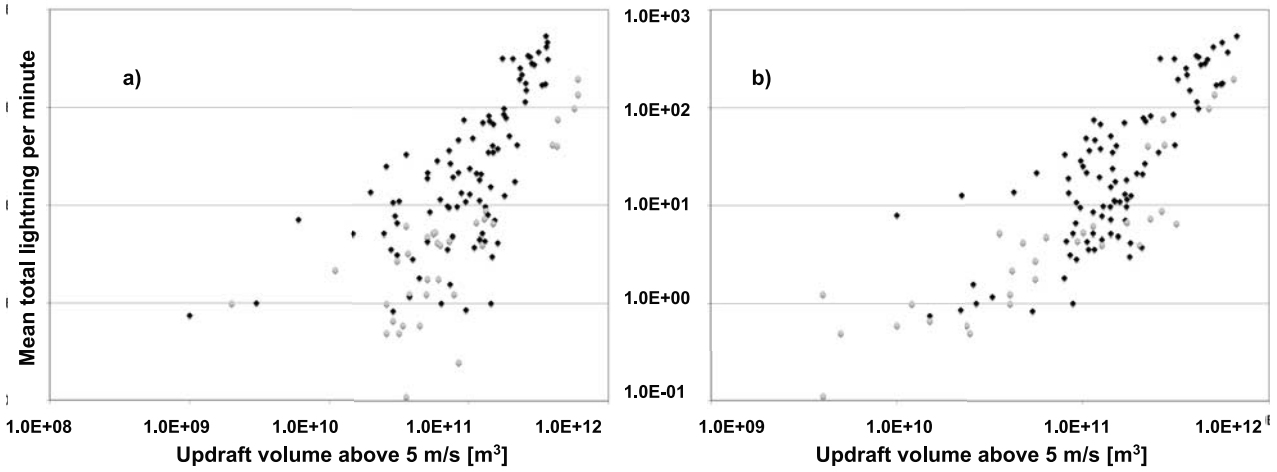

Figure 3. Updraft volume (m^3) at (a) 10°C < T < 0°C and (b) −20°C < T < −30°C with velocities greater than 5 m s^{-1} versus mean total lightning per minute averaged over the radar volume time for individual radar volumes of all 11 thunderstorms. The black dots mark data from the Colorado/Kansas High Plains, whereas the gray dots mark data from Northern Alabama.

Table 4. Linear Fit of Mean Total Lightning Per Minute Averaged Over the Radar Volume Time Versus Maximum Updraft Velocity (m^3) Between the −5°C and −40°C Level

	All Data Points	Data Points From Northern Alabama	Data Points From the Colorado/Kansas High Plains
Linear function	$f = 5.73w_{max} - 71.3$	$f = 4.4w_{max} - 424$	$f = 6.05w_{max} - 84.3$
Correlation (r)	0.8	0.68	0.8

the fact that the Alabama thunderstorm data points largely tend to overlay many of the High Plains data points in Figure 3b when colder temperatures are considered suggests that once the required updraft volume does exist above the melting level, precipitation ice production and conditions for charging may be similar for both regimes (cf. Figure 1). To the extent that the updraft volume impacts the ice water content production, this behavior seems generally consistent with the notion of regime–invariant relationships between precipitation ice water content and lightning flash rate as suggested by *Petersen et al.* [2005] and *Latham et al.* [2007].

[27] Contrasting the w_5 lightning results shown in Table 2 and Figures 2 and 3, we note a positive correlation between lightning flash rate and both the maximum (w_{max}) and the mean updraft (w_{mean}) ($r = 0.8$ and 0.65 respectively; Table 4). However, both of these correlations are lower than that demonstrated for lightning activity and w_5 (Table 2). A possible reason for the poorer correlation of both the maximum and mean updraft speeds, is that they do not necessarily represent the volume of updraft velocities involved in both microscale and macroscale charge separation. Figure 4 shows a scatter plot of w_{max} in the charging zone versus mean total lightning. A linear fit to the data points best represents the relationship between the w_{max} and lightning with a correlation coefficient of 0.8. The best-fit relationship is given in Table 4 together with separate linear fits to the data from the Northern Alabama and High Plains regions. The relationship between w_{max} and total lightning improved slightly at colder temperature layers similarly to w_5, but unlike w_5 w_{max} exhibited relatively invariant behavior as a function of climate regime for all temperature levels (not shown). Note that maximum updraft velocities (w_{max}) correlated slightly better to mean total lightning activity (Table 4) than mean updraft velocities (Table 2). Also the correlation between w_{max} and lightning was significantly higher for the storms over the Colorado/Kansas High Plains. This regional difference in the correlation between the maximum updraft and lightning may reflect a tendency for broader updrafts to coexist with updrafts of larger magnitude in the High Plains storms [e.g., *Musil and Smith*, 1989]. However, in contrast to the observations presented here, the modeling study of a High Plains supercell thunderstorm summarized in *Kuhlman et al.* [2006] noted a much smaller (order of magnitude) correlation between maximum updraft and lightning flash rate as compared with

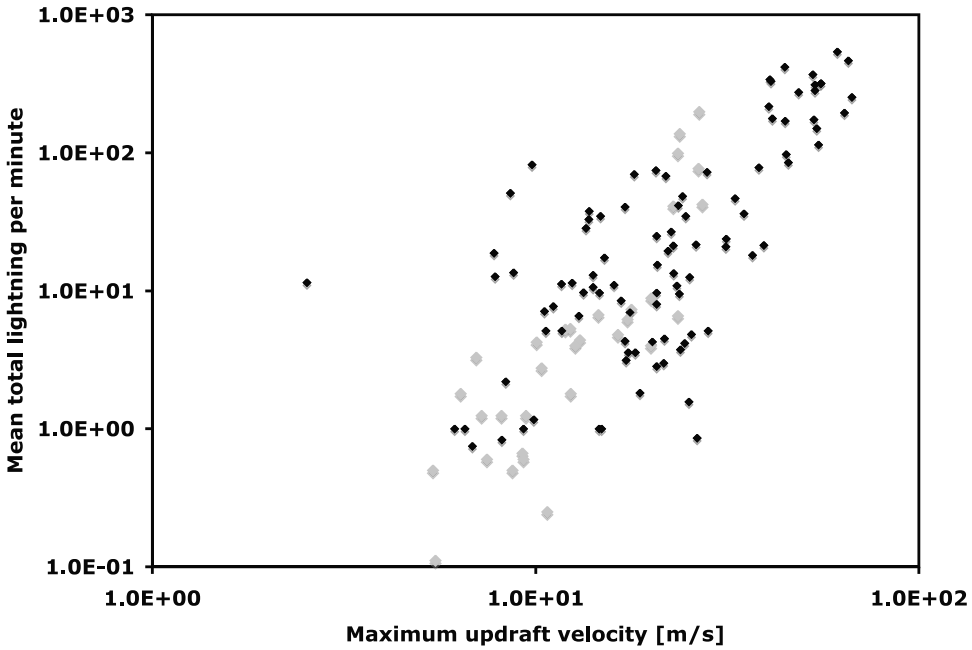

Figure 4. Maximum updraft speed (m s^{-1}) between the −5°C and −40°C levels versus mean total lightning per minute averaged over the radar volume time for individual radar volumes of all 11 thunderstorms. The black dots mark data from the Colorado/Kansas High Plains, whereas the gray dots mark data from Northern Alabama.

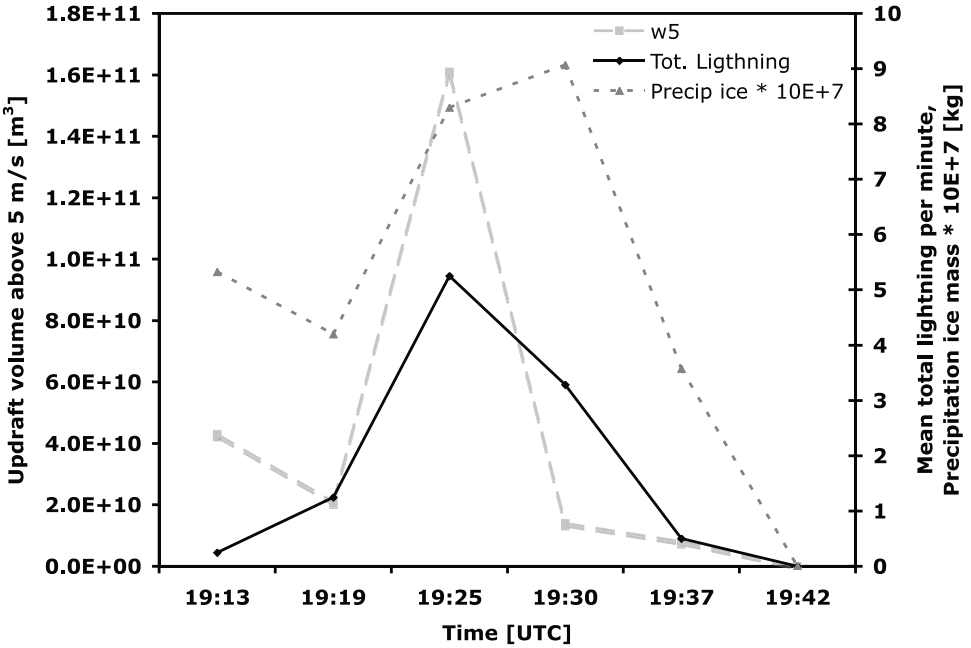

Figure 5. Mean total lightning rate per minute averaged over the radar volume time (solid black line), precipitation ice mass above the −5°C level (dotted gray line) and updraft volume (m^3) above the −5°C level with velocities greater than 5 m s^{-1} (w_5) of an ordinary single-cell thunderstorm that occurred on 13 July 2005.

that of updraft volume and flash rate. Collectively, these results emphasize an added relative importance of a more integrated quantity – the updraft volume (as opposed to considering only the characteristics of the maximum updraft) – to the development of lightning producing clouds.

[28] Note, that in addition we also investigated the relationship between total lightning and volume on a storm-by-storm basis. We found that updraft volume with $w > 5$ or 10 m/s generally follows the trend of total lightning well for the individual storms investigated herein. This is also true for the precipitation ice mass for temperatures colder than −5°C. As examples Figures 5 and 6 show the time series of w_5, precipitation ice mass for temperatures colder than −5°C and mean total lightning per minute for a

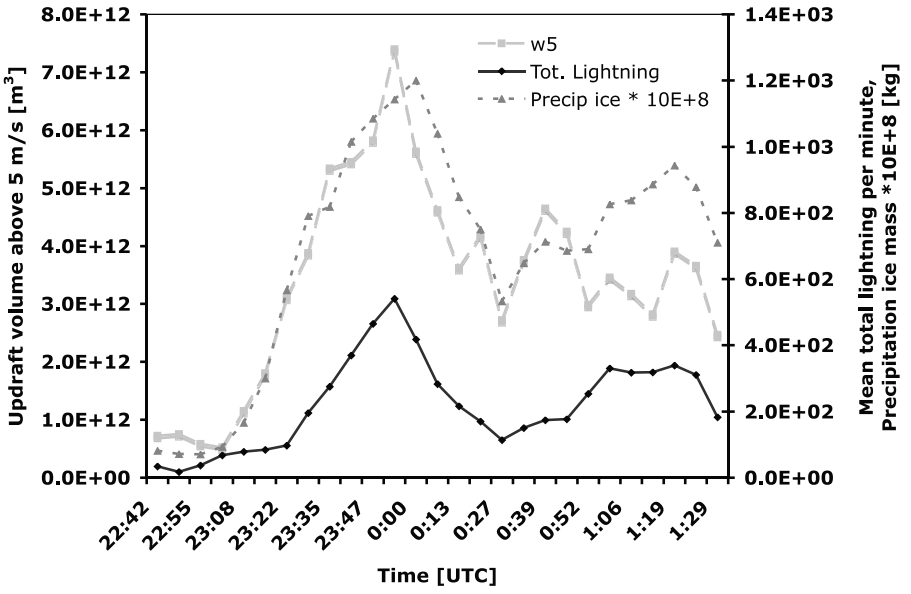

Figure 6. Mean total lightning rate per minute averaged over the radar volume time (solid black line), precipitation ice mass above the −5°C level (dotted grey line) and updraft volume (m^3) above the −5°C level with velocities greater than 5 m s^{-1} (w_5) of a supercell thunderstorm that occurred on 5 July 2000.

single cell storm that occurred on 13 July 2005 in northern Alabama and for a supercell storm that occurred during STEPS on 5 July 2000 respectively.

5. Conclusions

[29] This study used dual-Doppler radar data to evaluate the relationship between thunderstorm updraft characteristics and total lightning flash rate for a combination of eleven distinct thunderstorms of varying intensity and occurring in two different climate regimes (the subtropical southeastern U.S. and the High Plains). It is shown that the updraft volume above the −5°C level with vertical velocities greater than 5 and 10 m s^{-1} is well correlated to mean total lightning activity ($r = 0.93$ and $r = 0.92$ respectively). Neither the maximum, nor the mean updraft speeds in the charging zone correlated as well to total lightning activity ($r = 0.8$ or less) and these correlations varied by location.

[30] The relationship between updraft volume of the whole thunderstorm and total lightning activity varies as a function of temperature and, depending on the temperature, also with region. For the same lightning flash rate, southeastern U.S. thunderstorms were associated with a larger volume of updraft >5 m s^{-1} in the +10°C to 0°C layer compared to that observed in the High Plains thunderstorms. To some extent this is not surprising as the warm-cloud layer is typically, though not always, deeper in the southeastern U.S. than that found in the High Plains. Interestingly, as the cold-cloud active precipitation-based charging zone (e.g., temperature <−5°C) is approached the relationship between updraft volume and lightning flash rates becomes less regime variant, emphasizing the importance of cold cloud processes in lightning production and the similarity in thunderstorm behavior within the subfreezing temperature region of the noninductive charging zone.

[31] As mentioned in the introduction, it follows from scaling arguments summarized by *Boccippio* [2002] that the updraft area, and in particular, that area in the subfreezing layers of the cloud, should be related to the generator current density which in turn is linked to the electric activity of the storm. This conclusion is supported by results of this study. Large updraft volumes of ''higher'' updraft speeds are capable of producing more hydrometeors in the mixed ice phase region and thus higher number of collisions (between graupel and ice crystals) with subsequent charge separation.

[32] Though the results presented herein represent only a data sample from eleven storms, consistent with previous observational and modeling studies, the relationship between updraft volume *above the* −5°C *level* and total lightning was found to be robust and *very similar* for different storm types originating in two very different climate regions. From a remote sensing standpoint, since the updraft volume is related to cloud mass fluxes, precipitation mass, and diabatic heating, detection of total lighting activity in deep convection could also provide a continuous measurement proxy for updraft mass fluxes and the associated ice-phase precipitation in lightning-producing clouds [*Deierling et al.*, 2008]. With the impending deployment of a geostationary lightning mapper on the GOES-R series of satellites this can be especially useful. Furthermore, assimilation of similar information into mesoscale numerical models could improve predictions by pinpointing regions of enhanced cumulus mass flux during model initialization. Conversely, with expanded study designed to explore further regime variability (or lack thereof) of updraft volume–lightning flash rate relationships, better/refined parameterizations for the detection and prediction of lightning and/or prediction and diagnosis of storm intensity could be realized.

[33] **Acknowledgments.** We gratefully acknowledge the assistance and support of Dr. Hugh Christian and Dr. John Latham during the course of this work. We would also like to acknowledge Dr. Andrew Crook, Dr. Eric Defer, and Mr. Pat Kennedy for providing data sets and/or support in the data analysis.

[34] We also wish to acknowledge the sponsors funding this research, including the NASA Earth Observing Systems and Earth Systems Sciences Programs (TRMM-LIS; UAH-NASA Cooperative Agreement Contract NNM05AA22A), the NOAA GOES-R Global Lightning Mapper Risk Reduction Project (Dr. Petersen), a grant from NOAA supporting UAH Hazardous Weather Testbed activities (NA06-OAR4600156; Dr. Petersen), and the National Science Foundation Advanced Studies Program (Dr. Deierling).

References

Boccippio, D. J. (2002), Lightning scaling relations revisited, *J. Atmos. Sci.*, *59*(6), 1086–1104.

Bringi, V. N., G.-J. Huang, V. Chandrasekar, and T. D. Keenan (2001), An areal rainfall estimator using differential propagation phase: Evaluation using a C-band radar and a dense gauge network in the tropics, *J. Atmos. Oceanic Technol.*, *18*(5), 1810–1818.

Brunkow, D., V. N. Bringi, P. C. Kennedy, S. A. Rutledge, V. Chandrasekar, E. A. Mueller, and R. K. Bowie (2000), A description of the CSU-CHILL national radar facility, *J. Atmos. Oceanic Technol.*, *17*(12), 1596–1608.

Carey, L. D., and S. A. Rutledge (1996), A multiparameter radar case study of the microphysical and kinematic evolution of a lightning producing storm, *J. Meteorol. Atmos. Phys.*, *59*, 33–64.

Christian, H. J., et al. (1999), The lightning imaging sensor, in *11th International Conference in Atmospheric Electricity*, Guntersville, AL, 7–11 June, pp. 746–749.

Christian, H. J., Jr. (2008), The Geostationary Lightning Mapper Instrument for GOES-R, in *AMS 88th Annual Meeting*, New Orleans, LA, USA, 20–24 January 2008.

Crook, N. A., and J. Sun (2004), Analysis and forecasting of the low-level wind during the Sydney 2000 forecast demonstration project, *Weather Forecast.*, *19*(1), 151–167.

Defer, E., P. Blanchet, C. Thery, P. Laroche, J. E. Dye, M. Venticinque, and K. L. Cummins (2001), Lightning activity for the 10 July, 1996, storm during the stratosphere-troposphere experiment: Radiation, aerosol, and ozone-A (STERAO-A) experiment, *J. Geophys. Res.*, *106*(D10), 10,151–10,172.

Deierling, W., W. A. Petersen, J. Latham, S. Ellis, and H. J. Christian (2008), The relationship between lightning activity and ice fluxes in thunderstorms, *J. Geophys. Res.*, *113*, D15210, doi:10.1029/2007JD009700.

Dye, J. E., J. J. Jones, A. J. Weinheimer, and W. P. Winn (1989), Observations within two regions of charge during initial thunderstorm electrification, *Q. J. R. Meteorol. Soc.*, *114*(483), 1271–1290.

Dye, J. E., et al. (2000), An overview of the stratospheric–tropospheric experiment: Radiation, aerosols, and ozone (STERAO)-deep convection experiment with results for the July 10, 1996 storm, *J. Geophys. Res.*, *105*(D8), 10,023–10,046.

Goodman, S. J., et al. (2005), The North Alabama lightning mapping array: Recent severe storm observations and future prospects, *Atmos. Res.*, *76*(1–4), 423–437.

Jayaratne, E. R., C. P. R. Saunders, and J. Hallett (1983), Laboratory studies of the charging of soft hail during ice crystal interactions, *Q. J. R. Meteorol. Soc.*, *109*(461), 609–630.

Keeler, R. J., J. Lutz, and J. Vivekanandan (2000), SPol: NCAR's polarimetric Doppler research radar, in *Proceedings of the IEEE International Geoscience and Remote Sensing Symposium*, Honolulu, HI, 24–28 July, vol. 4, pp. 1570–1573, IEEE Catalog No. 00CH37120.

Kuhlman, K. M., C. L. Ziegler, E. R. Mansell, D. R. MacGorman, and J. M. Straka (2006), Numerically simulated electrification and lightning of the 29 June 2000 STEPS supercell storm, *Mon. Weather Rev.*, *134*(10), 2734–2757.

Lang, T. J., and S. A. Rutledge (2002), Relationships between convective storm kinematics, precipitation, and lightning, *Mon. Weather Rev.*, *130*(10), 2492–2506.

Lang, T. J., et al. (2004), The severe thunderstorm electrification and precipitation study, *Bull. Am. Meteorol. Soc.*, *85*(8), 1107–1125.

Laroche, P., A. Bondiou, P. Blanchet, and J. Pigere (1994), 3D VHF mapping of lightning discharge within a storm, paper presented at Foudre et montage 94, Chamonix, France.

Latham, J., W. A. Petersen, W. Deierling, and H. J. Christian (2007), Field identification of a unique globally dominant mechanism of thunderstorm electrification, *Q. J. R. Meteorol. Soc.*, *133*, 1453–1457, doi:10.1002/qj.133.

MacGorman, D. R., W. D. Rust, P. Krehbiel, W. Rison, E. Bruning, and K. Wiens (2005), The electrical structure of two supercell storms during STEPS, *Mon. Weather Rev.*, *133*(9), 2583–2607.

Mansell, E. R., D. R. MacGorman, C. L. Ziegler, and J. M. Straka (2005), Charge structure and lightning sensitivity in a simulated multicell thunderstorm, *J. Geophys. Res.*, *110*, D12101, doi:10.1029/2004JD005287.

Mansell, E. R., C. L. Ziegler, and D. R. MacGorman (2007), A lightning data assimilation technique for mesoscale forecast models, *Mon. Weather Rev.*, *135*(5), 1732–1748.

Marks, F. D., Jr., and R. A. Houze Jr. (1987), Inner core structure of hurricane Alicia from airborne Doppler radar observations, *J. Atmos. Sci.*, *44*(9), 1296–1317.

Matejka, T., and D. L. Bartels (1998), The accuracy of vertical air velocities from Doppler radar data, *Mon. Weather Rev.*, *126*(1), 92–117.

McCaul, E. W., Jr., K. M. Lacasse, S. J. Goodman, and D. Cecil (2006), Use of high resolution WRF simulations to forecast lightning threat, in *Preprints of the 23rd Conference on Severe Local Storms*, November 5–10, St. Louis, Missouri. CD-ROM, AMS.

Mohr, C. G., L. J. Miller, R. L. Vaughn, and H. W. Frank (1986), On the merger of mesoscale datasets into a common Cartesian format for efficient and systematic analysis, *J. Atmos. Oceanic. Technol.*, *3*(1), 143–161.

Musil, D., and P. Smith (1989), Interior characteristics at mid-levels of thunderstorms in the southeastern United States, *Atmos. Res.*, *24*(1), 149–167.

O'Brien, J. J. (1970), Alternative solutions to the classical vertical velocity problem, *J. Appl. Meteorol.*, *9*(2), 197–203.

Petersen, W. A., S. A. Rutledge, and R. E. Orville (1996), Cloud-to-ground lightning observations to TOGA COARE, selected results and lightning location algorithm, *Mon. Weather Rev.*, *124*(4), 602–620.

Petersen, W. A., S. A. Rutledge, R. C. Cifelli, B. S. Ferrier, and B. F. Smull (1999), Shipborne Dual-Doppler operations during TOGA COARE: Integrated observations of storm kinematics and electrification, *Bull. Am. Meteorol. Soc.*, *80*(1), 81–96.

Petersen, W. A., et al. (2005), The UAH-NSSTC/WHNT ARMOR C-band dual-polarimetric radar: A unique collaboration in research, education and technology transfer, in *Preprints of the 32nd AMS Radar Meteorology Conference*, Albuquerque, NM, 24–29 October. CD-ROM, AMS.

Reynolds, S. E., M. Brook, and M. F. Gourley (1957), Thunderstorm charge separation, *J. Meteorol.*, *14*(5), 163–178.

Rutledge, S. A., E. R. Williams, and T. D. Keenan (1992), The down under Doppler and electricity experiment (DUNDEE): Overview and preliminary results, *Bull. Am. Meteorol. Soc.*, *73*(1), 3–16.

Saunders, C. P. R., and S. L. Peck (1998), Laboratory studies of the influence of the rime accretion rate on charge transfer during crystal/graupel collisions, *J. Geophys. Res.*, *103*(D12), 13,949–13,956.

Saunders, C. P. R., W. D. Keith, and R. P. Mitzeva (1991), The effect of liquid water on thunderstorm charging, *J. Geophys. Res.*, *96*(D6), 11,007–11,017.

Sun, J., and N. A. Crook (1997), Dynamical and microphysical retrieval from Doppler radar observations using a cloud model and its adjoint. part I: Model development and simulated data experiments, *J. Atmos. Sci.*, *55*(12), 835–852.

Sun, J., and N. A. Crook (2001), Real-time low-level wind and temperature analysis using single WSR-88D data, *Weather Forecast.*, *16*(1), 117–132.

Takahashi, T. (1978), Riming electrification as a charge generation mechanism in thunderstorms, *J. Atmos. Sci.*, *35*(8), 1536–1548.

Takahashi, T., and K. Miyawaki (2002), Reexamination of riming electrification in a wind tunnel, *J. Atmos. Sci.*, *59*(5), 1018–1025.

Tessendorf, S. A., L. J. Miller, K. C. Wiens, and S. A. Rutledge (2005), The 29 June 2000 supercell observed during STEPS. part I: Kinematics and microphysics, *J. Atmos. Sci.*, *62*(12), 4127–4150.

Thomas, R., P. Krehbiel, W. Rison, J. Harlin, T. Hamlin, and N. Campbell (2003), The LMA flash algorithm, in *Proceedings of the 12th International Conference on Atmospheric Electricity*, Versailles, France, 9–13 June, pp. 655–656, ICAE.

Thomas, R., P. R. Krehbiel, W. Rison, S. J. Hunyady, W. P. Winn, T. Hamlin, and J. Harlin (2004), Accuracy of the lightning mapping array, *J. Geophys. Res.*, *109*, D14207, doi:10.1029/2004JD004549.

Vivekanandan, J., D. S. Zrnic, S. M. Ellis, R. Oye, A. V. Ryzhkov, and J. Straka (1999), Cloud microphysics retrieval using S-band dual-polarization radar measurements, *Bull. Am. Meteorol. Soc.*, *80*(3), 381–388.

Wiens, K. C., S. A. Rutledge, and S. A. Tessendorf (2005), The 29 June 2000 supercell observed during STEPS. part II: Lightning and charge structure, *J. Atmos. Sci.*, *62*(12), 4151–4177.

Williams, E. R., and R. M. Lhermitte (1983), Radar tests of the precipitation hypothesis for thunderstorm electrification, *J. Geophys. Res.*, *88*(C15), 10,984–10,992.

Workman, E. J., and S. E. Reynolds (1949), Electrical activity as related to thunderstorm cell growth, *Bull. Am. Meteorol. Soc.*, *30*, 142–149.

Zipser, E. J., and K. R. Lutz (1994), The vertical profile of radar reflectivity of convective cells: A strong indicator of storm intensity and lightning probability?, *Mon. Weather Rev.*, *122*(8), 1751–1759.

W. Deierling, National Center for Atmospheric Research, P.O. Box 3000, Boulder, CO 80301, USA. (deierlin@ucar.edu)

W. A. Petersen, ESSC/NSSTC University of Alabama in Huntsville, 320 Sparkman Drive, Huntsville, AL 35699, USA. (walt.petersen@nasa.gov)